

# F<sub>2</sub>-Laser Fabrication of Fiber-Integrated Optical Elements

Johannes ZINN, Manuel SCHÜTTE, Jörg MEINERTZ, Jürgen IHLEMANN

Laser-Laboratorium Göttingen, Hans-Adolf-Krebs-Weg 1, 37077 Göttingen, Germany

E-mail: juergen.ihlemann@llg-ev.de

F<sub>2</sub>-lasers with their vacuum-ultraviolet emission wavelength of 157 nm offer the possibility to process UV-transparent materials like quartz or fused silica by direct laser ablation. This way optical quartz fiber tips can be modified in a way that special beam characteristics of the fiber-emitted light are generated, i.e. the beam shaping optic is integrated into the fiber. Two ablation methods for this modification of fiber tips have been developed, lateral processing and axial processing. Both are based on mask projection in combination with a rotation of the fiber. Precise shaping of the tip with surface roughness around 30 nm is obtained. Examples of these fiber integrated optics are lenses, cones or inverted cones. These functional fiber tips can be applied in medical technology or metrology.

**Keywords:** F<sub>2</sub>-laser, fused silica, optical fiber, micro lens, mask projection, conical tip

## 1. Introduction

Optical fibers from fused silica are used in many kinds of applications ranging from communication and sensor technology to materials processing and medical surgery. In many cases the output of the fibers has to be adapted to the specific task. This can be an increase or decrease of the divergence angle, beam splitting or beam shaping. Conventionally, this is accomplished by external optical elements like ball lenses or gradient index (GRIN) lenses. This leads to rather bulky applicators, which often do not fulfill the requirements of miniaturization and ease of handling. Integration of the optical functionality into the fiber would be more compact, durable, and adjustment free; also it would minimize the number of optical surfaces. Thus, in this paper the fabrication of lenses and other optical components directly on the fiber tip is presented. For example, a convex lens integrated at the fiber tip will collimate or focus the emitted light. This opens up various possibilities of beam shaping required for medical or metrological fiber applications.

## 2. F<sub>2</sub>-laser processing of fused silica

Though ablation of fused silica is possible at standard excimer laser wavelengths (193 nm and 248 nm) [1], precise and reproducible results for multi-pulse nanosecond laser ablation have only been obtained at a wavelength of 157 nm [2,3]. Therefore, an F<sub>2</sub>-laser operating at this wavelength was used for the silica fiber processing. The applied optical beam delivery system, shown in fig. 1, is described in detail elsewhere [4]. Briefly, the output beam of an F<sub>2</sub>-laser (157 nm, 15 ns, 20 mJ, max. 200 Hz) is formed to homogeneously illuminate a mask, which is then imaged onto the work piece using a Schwarzschild-type reflective objective (demagnification 25x, numerical aperture NA = 0.4). The refractive optical elements are made from CaF<sub>2</sub> and the whole beam path is flushed with nitrogen to ensure high optical transmission at 157 nm, where fused silica and oxygen would completely absorb the beam.

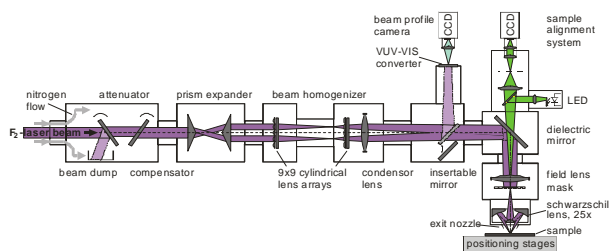


**Fig. 1** F<sub>2</sub>-laser beam-shaping and mask-projection optics

## 3. Lateral processing of fiber lenses

The first method (*lateral processing*) is based on a mask projection arrangement perpendicular to the fiber axis [5,6]. The scheme of this arrangement is shown in fig. 2.

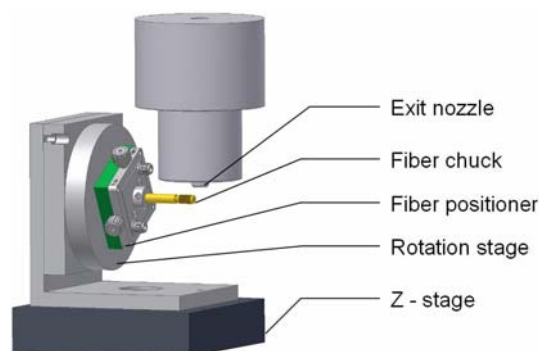


**Fig. 2** Set-up for lateral fiber processing. Beam path: top down

The fiber is rotated around its axis while the laser cuts through the fiber, yielding a rotationally symmetric tip with a shape defined by the mask aperture. Among other shapes, convex lenses (spherical or aspherical) can be fabricated this way. Fibers with small and medium diameters can be treated in one exposure. As the processing field is limited

to  $200 \times 200 \mu\text{m}^2$ , large-diameter fibers have to be processed in several steps. Therefore, a conformal mask- and fiber displacement was introduced, so that by a step and repeat mode thick fibers can be processed without significant stitching errors (fig. 3).

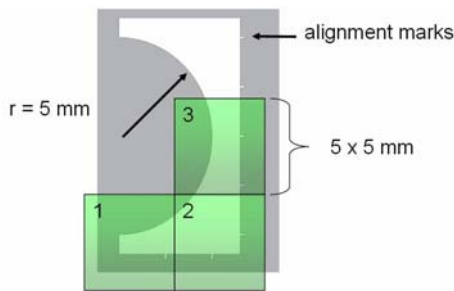


**Fig. 3** Step and repeat processing of thick fibers. Areas 1 to 3 are processed sequentially. The mask is demagnified 25x.

This way, fibers with core diameters of  $400 \mu\text{m}$  or more can be processed very precisely (Fig. 4). For this kind of lateral processing no pretreatment like cleaving or polishing is necessary, because the resulting shape does not depend on the original fiber surface, but only on the precision of centering of the fiber on the rotation axis and on the precisely correlated displacement of mask and fiber between the processing steps.

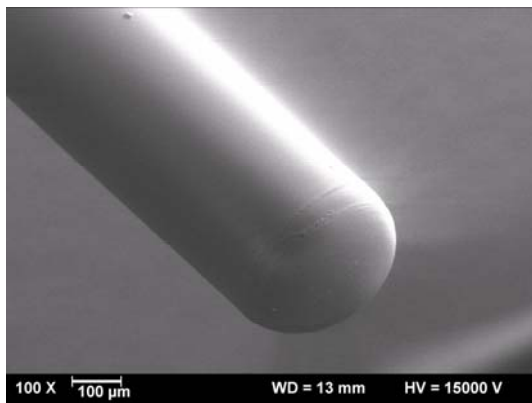


**Fig. 4**  $F_2$ -laser processed fused silica fiber tip. Lateral processing of a  $400\mu\text{m}$ -fiber using conformal mask imaging (cf. fig. 3). Fluence:  $5\text{J}/\text{cm}^2$

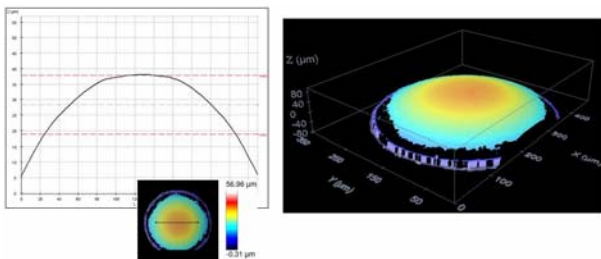


**Fig. 5** Confocal microscope image (objective 50x,  $\text{NA} = 0.8$ , vertical resolution:  $200 \text{ nm}$ ) of a lens on a  $400\mu\text{m}$ -fiber (cf. fig. 4).

Fig. 5 displays a confocal microscope image taken from a lens on a  $400\mu\text{m}$  fiber. A smooth surface without any steps that would arise from imperfect stitching is observed.

A surface roughness of  $R_a \approx 30 \text{ nm}$  has been measured by atomic force microscopy.

To characterize the focusing performance of the fiber lenses, a HeNe-laser beam was coupled into the fiber at the opposite side, and the cross sections of the output through the lens were recorded with a CCD-camera (fig. 6). To do this, a microscope objective ( $20\times$ ,  $\text{NA} = 0.5$ ) was used to image planes with varying distance from the fiber tip (fig. 7).

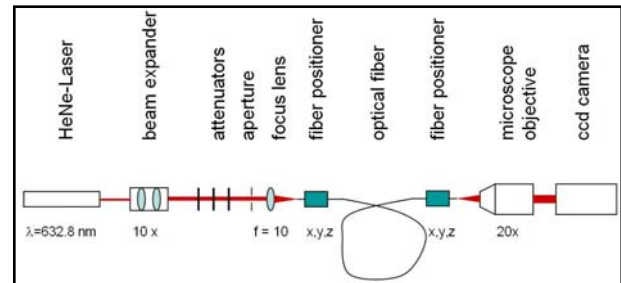


**Fig. 6** Experimental setup to measure the output characteristics of a fiber lens.

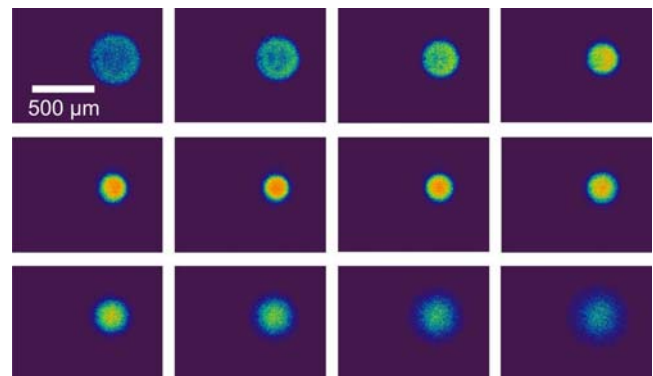


**Fig. 7** Beam profile of a fiber lens with a radius of curvature of  $200 \mu\text{m}$  on a  $400\mu\text{m}$ -diameter fiber. The images show the beam profile behind the objective while moving the fiber in front of the objective. The increment of the distance is  $0.1 \text{ mm}$  for each image.

The obtained data of the focal spot size and the focal distance for various lenses are shown in table 1.

**Table 1** Characteristics of fiber lenses on  $400\mu\text{m}$ -fibers

Radius of lens curvature	Focal spot size (4x std. dev.)	Focal distance
$200 \mu\text{m}$	$240 \mu\text{m}$	$160 \mu\text{m}$
$250 \mu\text{m}$	$300 \mu\text{m}$	$150 \mu\text{m}$
$300 \mu\text{m}$	$310 \mu\text{m}$	$150 \mu\text{m}$

Thus, a spot of  $240 \mu\text{m}$  diameter can be obtained at a distance of  $160 \mu\text{m}$  from the fiber output compared to a cross section of about  $500 \mu\text{m}$  in the case of the bare fiber at the same distance.

#### 4. Axial fiber processing

In the second technique (*axial processing*), the mask is projected onto the front face of the fiber. Precise cleaving

or polishing prior to laser processing is required to obtain good results. To fabricate lenses or other rotational symmetric elements by this method, in a basic version a pin-hole or another defined aperture is used as mask. The generated laser spot on the fiber face is steered along a trajectory of overlapping concentric circles by rotating the fiber. The generated profile is controlled by the spot size, the number of circles in the trajectory, and the scanning speed [6]. This axial method was extended to the use of special shapes of the mask. By choosing a slit or an “inverted slit” (opaque bar in transparent environment) in the mask position, conical tips can be fabricated (Fig. 8a). Variation of the width of the slit and its displacement with respect to the rotation axis can be used to fabricate various shapes.

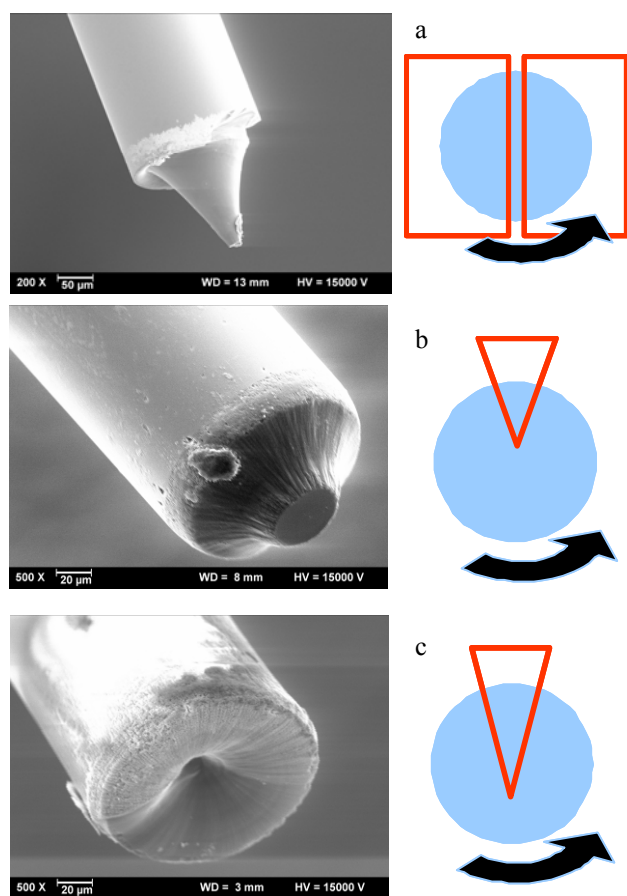


**Fig. 8** Various conical fiber tips. The red-bordered areas denote the open mask field; the blue circle denotes the rotating fiber end face.

Using a triangular mask aperture which is generating a triangular spot on the outer rim of the fiber end face, a truncated cone is fabricated (fig 8b). If the center of the fiber end face is covered by the triangular laser spot like in fig 8c, an inverted cone is generated. An even larger variety of (asymmetric) shapes can be fabricated, if the rotation axis is different from the fiber axis.

### 5. Fiber tip gratings

By projecting a grating mask onto the (non-rotating) fiber end face in the axial configuration, fiber tip gratings can be formed. Similarly to the fabrication of linear gratings [3], two-dimensional gratings are obtained imaging a

mesh like mask. Such a grating will act as a diffractive beam splitter for the fiber output. The intensity distribution in the different spots can be varied by adjusting the duty cycle of irradiated and non-irradiated areas and the depth of the ablated grooves. Fig. 9 displays such a crossed fiber grating, and fig. 10 shows that for this grating there is a strong zero order spot and weaker spots in the first and mixed orders. Also, in fig. 9 one can see the different ablation depths of various materials. While the silica core is perfectly patterned at its surface, the hard polymer cladding and the Tefzel coating are ablated at the same fluence more deeply with lower contrast forming a groove around the core.

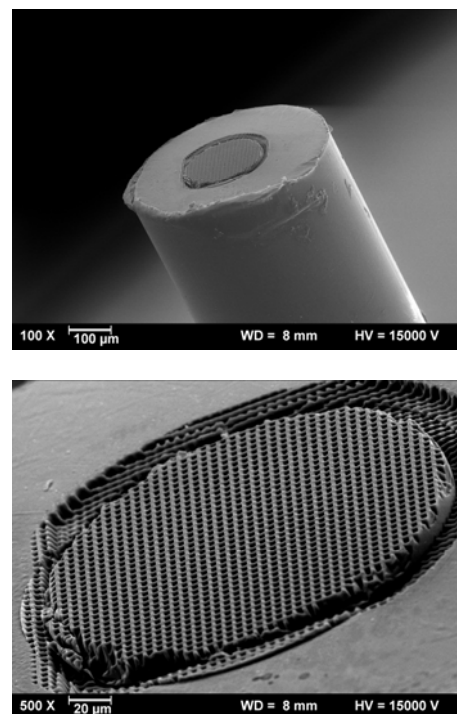


**Fig. 9** Crossed grating on a 200 $\mu$ m-core fused silica fiber to be used as beam splitter. Process parameters: 4.5 J/cm<sup>2</sup>, 32 pulses.

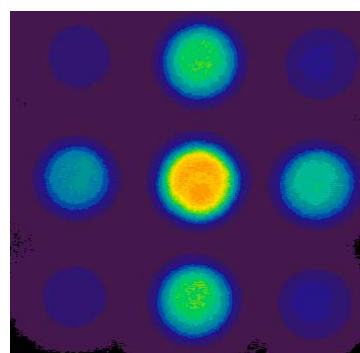


**Fig. 10** Measured beam profile of the fiber output generated by the crossed grating shown in fig 9.

### 6. Conclusion

F<sub>2</sub>-laser ablation enables precise processing of fused silica with optical surface quality. Fiber-integrated optics like lenses, gratings, and cones can be fabricated by this method. Applications in sensor technology and medical technology are possible.

### **Acknowledgments**

Financial support by the German Ministry of Economy and Technology is gratefully acknowledged (Grant no. 16IN0351).

### **References**

- [1] J. Ihlemann, *Appl. Surf. Sci.* **54**, 193 (1992).
- [2] P.R. Herman, R.S. Majoribanks, A. Oettl, K.P. Chen, I. Kononov, S. Ness, *Appl. Surf. Sci.* **154-155**, 577 (2000).
- [3] J. Ihlemann, S. Müller, S. Puschmann, D. Schäfer, M. Wei, J. Li, P.R. Herman, *Applied Physics A* **76**, 751 (2003).
- [4] P.R. Herman, K.P. Chen, M. Wei, J. Zhang, J. Ihlemann, D. Schäfer, G. Marowsky, P. Oesterlin, B. Burghardt, *Proc. SPIE Vol.* **4274**, 149 (2001).
- [5] J. Li, J. Dou, P.R. Herman, T. Fricke-Begemann, J. Ihlemann, G. Marowsky, *Journal of Physics: Conference Series* **59**, 691-695 (2007).
- [6] T. Fricke-Begemann, J. Li, J. Dou, J. Ihlemann, P.R. Herman, G. Marowsky, *Proc. of the Third International WLT-Conference Lasers in Manufacturing, LIM 2005*, pp. 733-737 (2005).

(Received: July 9, 2009, Accepted: December 3, 2009)